Efficient Low Cost Range-Based Localization Algorithm for Ad-hoc Wireless Sensors Networks

Mohamed Shaheen Elgamel, Abdulhalim Dandoush

Efficient Low Cost Range-Based Localization Algorithm for Ad-hoc Wireless Sensors Networks

Mohamed Elgamel and Abdulhalim Dandoush
cshaheen@hotmail.com, abdulhalim.dandoush@inria.fr*

University of Louisiana at Lafayette
P.O. Box 43004
Lafayette, LA 70504 USA

*INRIA Sophia-Antipolis Méditerranée
2004 Route des Lucioles BP93
06902 SOPHIA ANTIPOLIS, France

Abstract

Building an efficient node localization system in wireless sensor networks is facing several challenges. For example, calculating the square root consumes computational resources and utilizing flooding techniques to broadcast nodes location wastes bandwidth and energy. Reducing computational complexity and communication overhead is essential to reduce the power consumption, extend the life time of the battery operated nodes, and improve the performance of the limited computational resources of these sensor nodes. Localization algorithms can be classified as range-free or range-based Algorithms. Range-based algorithms are more accurate but also more computationally complex. However, in applications such as target tracking, localization accuracy is important. In this paper, we revise the mathematical model,the analysis and the simulation experiments of the basic Trigonometric based Ad-hoc Localization System (TALS), a range-based localization system presented previously. A better picture on the overall behavior of TALS is drown. Furthermore, the study is extended, and a new technique to optimize the system is proposed. A deep analysis and an extensive simulation for the optimized TALS is presented showing its cost, accuracy, efficiency, and deducing the impact of its parameters on the performance. Thus, the contribution of this work can be summarized as follows: 1) Extending and optimizing the basic TALS that reduces the computational overhead by eliminating the need of solving a linear system of equations via least square methods and its variants or the need to any square root operations. 2) Revision of the system formulas and providing correct and accurate equations 3) Deeply analyzing, and extensively simulating the optimized TALS showing its cost, accuracy, efficiency, and deducing the impact of its parameters, such as the initial anchors density, the number of considered localizing neighbors aiding in the localization process, the transmission noise, and noisy measurements, on the performance. 4) Ensuring a very good accuracy with less complexity than the basic TALS by proposing and using a novel modified Manhattan distance in the elimination process. Through the mathematical analysis and intensive simulation, the optimized TALS has presented superior performance and accuracy results compared to other localization techniques.

Keywords: Wireless Sensor Networks, WSNs, Range-based Localization, Distributed Localization, Anchor-based Localization, Simulation, distance measure, Modified Manhattan, Performance Evaluation

*Corresponding author

1. Introduction and motivation

The advancement of embedded systems and wireless communication brought forth wireless sensor networks (WSN). These wireless sensor devices are deployed in plethora of applications ranging from civil solutions to military applications. Target localization and real time target tracking are widely adopted applications for wireless sensors networks. Possessing the knowledge of the node's location is a key parameter in these applications and in several routing algorithms [1]. The ad-hoc nature of the sensor devices makes self-positioning an integral part of their applications.

The basic idea used in a node localization system is to measure a physical quantity, e.g. signal strength, that is proportional to distance and use the measured value to estimate the distance to a reference point. Once the distance is known to at least three reference points, the position of the tracked node can be determined.

Thus, the WSN localization process consists typically of three phases (*i*) coordination (e.g. clock synchronization, notification of the need to localize a position) [2, 3], (*ii*) measurement of a physical quantity (transmission of a signal followed by signal processing), and (*iii*) position estimation [4]. Initializing a localization process requires the coordination of some nodes. One or more nodes then emit a signal, and some property of the signal (e.g. arrival time, phase, signal strength, etc.) is observed by one or more receivers. Next, to determine the location of a node, signal measurements have to be transformed into position estimates by means of a localization algorithm. As mentioned previously, to achieve these phases correctly, the existence of cooperating sensor nodes that have been deployed into the environment at known positions a priori is essential. These nodes are called reference points or anchor nodes. The location of an anchor node is known either through a Global Positioning System (GPS), manually predefined, or calculated during the localization system operations.

Building an efficient node localization system in wireless sensor networks is facing several challenges. For example, reducing communication overhead in the two first phases of the localization process and computational complexity in the third phase is essential to reduce the power consumption, extend the lifetime of the battery operated nodes and improve the performance of the limited computational resources nodes. Typically, deployments of WSNs exist in harsh environments where nodes are subject to high measurement errors due to instrumentation and communication noise. Moreover, WSN nodes are subject to destruction due to environmental effects and batteries running out. To address these challenges and overcome the problems of measurements errors and communication noises of sensor nodes, redundancy of sensor nodes and information fusion are of great use and are employed in several WSN applications. Node redundancy and information fusion techniques can enhance the quality of the estimates by avoiding outliers and substitute for missing information caused by network congestion.

The following is a summary of the challenges in building a node localization system

- Flooding: Anchor nodes flood the network with their positions which waste energy and bandwidth communication [5].
- Solving a linear system of equations: A system of linear equations is solved using least square approximations which pose a huge computational overhead [6].
- Finding shortest path: Computing the shortest path between anchor nodes to infer ranging estimates which wastes communication bandwidth [5].
- Square root operations: A computational intensive task that does not suit WSN devices.
- High erroneous measurements: That poses a threat on the accuracy of the estimation process.

Therefore, proposing novel simple methods that can improve the localization accuracy with low cost is still a research challenge. In a preliminary joint work in [7], TALS is proposed to address the above challenges. TALS is an anchor based localization system to address the current

existing localization systems deficiencies. It utilizes ranging measurements, trigonometric functions, square distance comparisons. Moreover, a data fusion technique is applied to the different redundant estimates of each node to come out with one accurate estimate of the node location. Nodes that have estimated their location are upgraded to become anchor nodes and aid in the localization algorithm. In this study we introduce a novel distance measurement technique to the TALS localization system, that can be seen as a modified Manhattan (MM) distance measurement technique. MM is used in calculating and comparing two distances as the system under consideration does not care about the exact distance calculation. It does care about which estimated point is closer to the actual one in order to move to. The optimized TALS localization system is modeled and its performance is evaluated.

In this paper, we revise the mathematical model of the system, the analysis and the simulation experiments of the basic TALS in [7] so that we show a better picture on the overall behavior of TALS. Furthermore, we extend the study, optimize the system and present a deep analysis and an extensive simulation for the optimized TALS showing its cost, accuracy, efficiency, and deducing the impact of its parameters on the performance. Thus, the contribution of this work can be summarized as follows:

1) Extending and optimizing the basic Trigonometric based Ad-hoc Localization System (TALS) [7] that reduces the computational overhead by eliminating the need of solving a linear system of equations via least square methods and its variants or the need to any square root operations. 2) Revision of the system formulas and providing correct and accurate equations 3) Deeply analyzing, and extensively simulating the optimized TALS showing its cost, accuracy, efficiency, and deducing the impact of its parameters on the performance. 4) Ensuring a very good accuracy with less complexity than the basic TALS by proposing and using a novel modified Manhattan distance in the elimination process.

1.1. Paper Organization

The rest of the paper is organized as follows. In Section 2, the related work in sensor network localization issues is discussed. Section 3 discusses the TALS algorithm in details and presents the Modified Manhattan distance measurement technique to optimize the elimination process; the core process in TALS. The section proposes also a data fusion techniques to optimize TALS results. The analysis of the TALS algorithm and the effect of different parameters on the localization process are provided in Section 4. Section 5 describes the simulation environment and presents the results of extensive simulation of the optimized TALS while showing its cost, accuracy and efficiency. The impact of the system parameters on the performance is deduced also. Section 6 presents the conclusion and future work.

2. Related Work

Although the literature on localization methods for WSNs is abundant [6–21], proposing novel simple methods that can improve the localization accuracy with low cost is still a research challenge and an important issue for several applications in many domains such as commercial, environmental, health, and military domains [8, 9, 10, 11].

Several localization algorithms exist in literature where many of them depend on variations of Lateration, Trilateration, Multilateration, Angulation or Cellular Proximity. Localization algorithms can be classified as range-free or range-based. Range-based algorithms are more accurate but also more computationally complex. Range-based methods require at least 3 localized nodes (4 in a 3-D setting) to enable localization of a fourth node with varying degrees of quality. The position of wireless nodes can be determined using one of five basic techniques, namely time of arrival (TOA) [6], time difference of arrival (TDOA) [12, 13, 14, 15], angle of arrival (AOA) [16], Hop-count or received signal strength (RSS) [17, 18], [19], [20]. Range-based approaches give in general high localization accuracy in the expense of extra hardware and complexity.

The range-free methods are based on the use of the topology information and connectivity such that they ignore the use of range measurement techniques [21]. These later methods may use

variations of one hop distance victor (DV-HOP) [22, 23], an Approximate Point-In-Triangulation test (APIT) [24], Centroid [25], or multidimensional scaling (MDS-MAP) [26]. Those localization schemes are characterized, on one hand, by their simplicity , ease of implementation, but on the other hand, they have bad localization accuracy [27, 28].

Anchor-based range-based localization techniques estimate locations usually by solving a set of linear equations using least square approximation or any of its variants. Niculescu and Nath have proposed the APS system in [5] that is an anchor based localization system that utilizes ranging measurements. APS estimates ranges across several hops from the node being localized by finding the shortest path between the anchor nodes and the positioning node. APS utilizes these computed ranges to compute the location of the nodes using a simplified version of the GPS algorithm (see [29] for more details about GPS). The algorithm starts with an initial estimate, and iteratively solves a system of linear equations until the threshold is met. There are several disadvantages for using this technique. APS utilizes flooding techniques to compute the shortest distance from the anchor nodes to each node in the network and to broadcast their positions. This overhead in communications wastes power and time. Furthermore, APS iteratively tries to solve a system of linear equations using least square approximation which presents an overhead in computations. Savvides et al. used the iterative atomic multilateration technique based on TOA in [6] to estimate the location of the nodes. The estimation is calculated by solving a system of linear equation using MMSE [30], when a node has three or more anchor nodes as neighbors. Each node that has computed its estimated location becomes an anchor node and aids in the localization of the rest of the network in an iterative manner. This technique suffers from the complexity residing in solving a system of linear equation which has a complexity of $O(n^3)$ [31]. In [17, 18] the Received Signal Strength RSS Indicator approach is used to localize position of unknown nodes. This technique is based on the physical fact of wireless communication that theoretically, the signal strength is inversely proportional to the squared distance between a pair of sensor nodes. A known radio propagation model is used to convert the received signal strength into distance.

Thus, the TOA and TDOA schemes can achieve high localization accuracy but they require extra hardware and therefore more energy consumption. Among the range-based measurement techniques, the RSS technique is the most common techniques, cheapest and simplest, because it does not require additional hardware. However, it is very susceptible to noise and obstacles, particularly for indoor environment. It requires also more data compared with other methods to achieve higher accuracy as it should consider errors in the measured values, which can be obtained from multi-path propagation, fading effects and reflection. Moreover, extending a RSS-based technique for 3D localization can introduce higher complexity in computational cost and location accuracy [27].

In our previous joint work, Merhi et al. [32], the 7 point trilateration technique is designed to perform acoustic target localization. Later, this technique has been used in our preliminary joint work in [7] to perform reasonable low cost and accurate node localization. In fact, the 7 point trilateration technique is a range-based anchor-based localization scheme that solves the system of linear equations using geometric representations. As mentioned in Section 1, the objective of [7] was to build a reliable, efficient, and low cost localization system that uses ranging measurements, trigonometric functions, square distance comparisons and a data fusion technique. TALS proved to be a promising localization system that one can build on it for providing efficiency and localization accuracy to many WSN applications. We aim in this work to employ a novel modified Manhattan (MM) distance measurement technique in TALS instead of the square distance comparison technique in order to provide a more lower cost and simple range-based anchor-based localization system. We will analyze in depth the performance of the system and we will assess the effects of the different parameters on the efficiency and accuracy.

3. TALS Algorithm

3.1. Overview

In this section, we describe anchor based localization algorithm that utilizes range measurements, which is called TALS. Initial Anchors have their pre-known accurate positions. They are equipped with GPS. Each node is assumed to be capable of generating a distance estimate to any of its one-hop neighbors. However, nodes are only required to estimate ranges between its location and the anchor nodes. Typically, ranging estimates are performed by one of the four basic techniques. Initially, the algorithm starts by anchor nodes transmitting their own locations to their one hop neighbors. Each node that receives more than two anchor locations will start the localization process. Each node will select an anchor node at random and chooses it as a base. The node's estimated position lies on a circle centered at the base anchor node's location with a radius $\tilde{d}$ which is the estimated range to the node being localized as shown in Fig. 1(a). The challenge arises in determining which point on this circle is the estimated position and in which quadrant this point exist. Thus, an elimination process is proposed and employed as in the next sub-section.

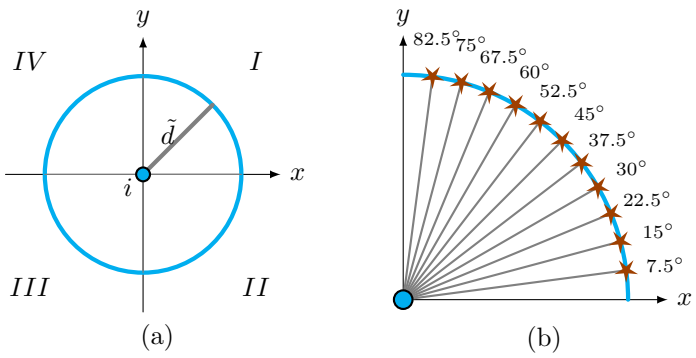

Figure 1: TALS generation of estimate points

3.2. TALS: basic elimination process

First, the basic simple, low cost and efficient TALS elimination process is described. Second, an additional enhancement and optimization in term of computation cost and complexity while conserving the accuracy level is introduced.

First of all, the circle is divided into points as shown in Fig. 1(b), where each point could be a potential estimate and we will refer to it as an estimate point. The division is done uniformly across all quadrants of the circle where only the division of quadrant I is shown in Fig. 1(b). The angle degree for which the circle is divided is a design parameter that will be discussed in Sec. 4.2.

To choose which point on this circle is the best estimate and eliminate the others candidate points, additional anchor nodes aid in the localization process. We define $\mathbb{A}$ as the set of these additional anchor nodes. The elimination or the selection is done by comparing the squared estimated range of the node being localized to the squared distance from the additional anchor nodes to the points on the circle through multiple iterations. The elimination process starts by choosing which quadrant the estimate lies on. As shown in Fig. 2(a), consider the base anchor node i and two other anchor nodes $l \in \mathbb{A} = \{j, k\}$. The algorithm starts initially by selecting four points which lie on the circle of node i at 45° from the x-axis as shown in Fig. 2(b,c).

The coordinates of the first estimate point in quadrant I can be calculated using the following equations:

$$\tilde{x}_{45I} = x_i + \tilde{d}_i \, cos\alpha, \; where \; \alpha = 45 \tag{1}$$

$$\tilde{y}_{45I} = y_i + \tilde{d}_i \, sin\alpha, \; where \; \alpha = 45; \tag{2}$$

The three other estimate points that lie on the other three quadrants can be populated using trigonometric properties:

$$\tilde{x}_{45II} = \tilde{x}_{45I} \quad , \quad \tilde{y}_{45II} = -\tilde{y}_{45I} \tag{3}$$

$$\tilde{x}_{45III} = -\tilde{x}_{45I} \quad , \quad \tilde{y}_{45III} = -\tilde{y}_{45I} \tag{4}$$

$$\tilde{x}_{45IV} = -\tilde{x}_{45I} \quad , \quad \tilde{y}_{45IV} = \tilde{y}_{45I} \tag{5}$$

But as each sensor to be localized will take a basic anchor as the reference for its measurements, we need to adapt the previous equations as below:

$$\tilde{x}_{45II} = \tilde{x}_{45I} \tag{6}$$

$$\tilde{x}_{45III} = \tilde{x}_{45IV} = x_i - \tilde{d}_i \, cos\alpha \tag{7}$$

$$\tilde{y}_{45IV} = \tilde{y}_{45I} \tag{8}$$

$$\tilde{y}_{45II} = \tilde{y}_{45III} = y_i - \tilde{d}_i \, sin\alpha \tag{9}$$

The node will compute (in the basic TALS) the squared distance from anchor j and k to the 4 points using the following equations (see Fig. 2(b,c)):

$$\tilde{d}^2_{j45m} = (x_j - x_{45m})^2 + (y_j - y_{45m})^2 \tag{10}$$

$$\tilde{d}^2_{k45m} = (x_k - x_{45m})^2 + (y_k - y_{45m})^2 \tag{11}$$

for m=I, II, III and IV

The above values are compared against the estimated ranges $\tilde{d}^2_j$ and $\tilde{d}^2_k$ respectively by taking the absolute difference as follow:

$$\tau_m = |\tilde{d}^2_k - \tilde{d}^2_{k45m}| + |\tilde{d}^2_j - \tilde{d}^2_{j45m}| \tag{12}$$

for m=I, II, III and IV, the name of a quadrant.

The point that has the lowest residue τ resulting from taking the sum of absolute differences is the point that is the nearest to the node and hence the quadrant is selected as shown in Fig. 2(d). This is due to the fact that for two-dimensional localization, we need usually three anchor nodes (three range measurements from known positions). Each range can be represented as the radius of a circle, with the anchor node situated at the center. Without measurement noise, the three circles would intersect at exactly one point, the location of the target node. Note that we don not solve a linear system of equations and we don not use square root functions.

The reason why the squared distance is used in (10), (11) and (12) lies in the fact that square root functions are expensive in terms of computational complexity. In this way, these functions are eliminated and are substituted for them by squared functions that improves the performance without reducing the accuracy. As shown in Fig. 5, the second iteration of the elimination process starts by selecting two new estimate points into the selected quadrant, e.g. quadrant I in this example, located at $\pm 15°$ to/from the first selected point that was lying on 45° in our example. That is, the two estimate points lie on the circle of node i at 30° and 60° from the x-axis as shown in Fig. 5. The coordinates of these two estimate points are calculated using equations (1) and (2) by substituting for α by 30° and 60°. The squared distance to these two points are then computed using the following equations.

$$\tilde{d}^2_{a30} = (x_a - x_{30})^2 + (y_a - y_{30})^2, \quad \forall a \in \mathbb{A} \tag{13}$$

$$\tilde{d}^2_{a60} = (x_a - x_{60})^2 + (y_a - y_{60})^2, \quad \forall a \in \mathbb{A} \tag{14}$$

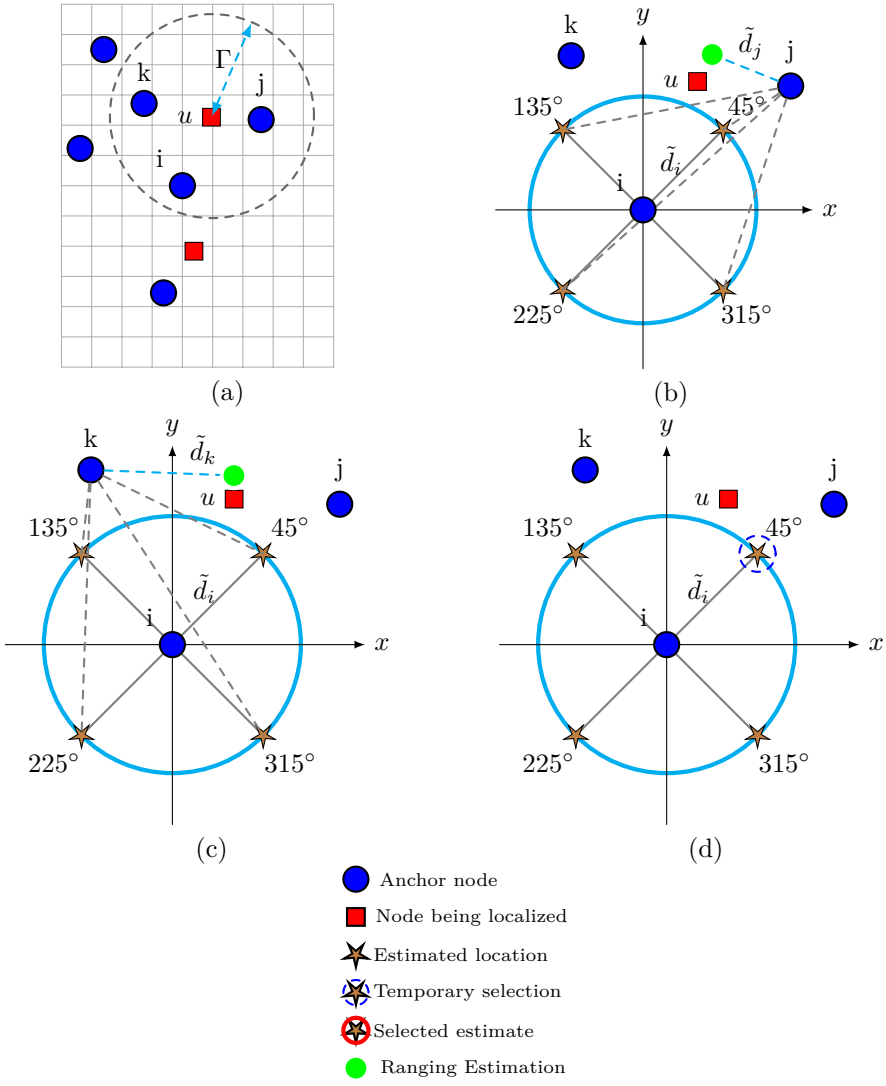

Figure 2: TALS generation of estimate points.

Subscript a in equations (13) and (14) refers to the anchor node aiding in the localization process. The computed values are again compared against the estimated range where the point with the lowest residual τ is selected. If at any time the residual τ is smaller or equal to the threshold ξ, the elimination process stops and the point with the lowest residual is selected as the final estimate. The process continues iteratively in a binary-search like manner until the threshold condition is satisfied. For an example, if point 60° is selected and the threshold condition is not met, the third elimination phase selects the two points (52.5° and 67.5°) such that the comparison will be between them as shown in Fig. 5(d,e,f). The selection of the estimate points is done using the equation $p \pm \frac{15^\circ}{i}$, where p represents the location of the first estimate point ($p = 45^\circ$ in our example) and i stands for the phase number of the elimination process. The algorithm stops when the threshold condition is met or when the divisions reach 0° or 90°.

3.3. Optimization for the elimination process using a novel modified Manhattan distance

In this section, we propose a novel distance measurement technique for computing the residue τ that indicates through (12) the nearest estimate point in each iteration phase to the real position of the node being localized. To address this enhancement, we will use a novel Modified

Manhattan Distance technique instead of the squared distance through all the iterations of the elimination process. Let us first review the distance measurement techniques and then proceed to the introduction of the novel Modified Manhattan Distance technique and its use in TALS.

Concerning the distance measurement techniques, several methods can be applied in different domains or applications to measure the distance to the nearest base node or to measure the distance between two points or to express similarity/dissimilarity between pairs of objects. One of the most popularly used distance measures is Minkowski distance that is expressed in Equ. (15). Manhattan (or city block) distance and Euclidean distances are specialized versions of Minkowski distance and are the most offten used ones. These techniques are used in many fields such as image retrieval, Gabor Jets-based Face Authentication (face recognition systems) , similarity measurement for motion tracking in a video sequences, estimation of location in WSN [17, 18], clustering analysis, and in the localization process in WiFi AP range [33].

Henceforth, $d(.)$ is used to denote the basic distance function and $dist(.)$ will be used to denote the distance function of the complex construct. Given two vectors u and v of the same length $N \geq 1$, Minkowski distance is computed as follows:

$$dist(u,v) = Minkowski_p(u,v) = \sqrt[p]{\sum_{i=1}^{N} d(u_i,v_i)^p} = \sqrt[p]{\sum_{i=1}^{N} |u_i - v_i|^p} \tag{15}$$

where p is the order of Minkowski distance. Manhattan distance is a special case of Minkowski when $p = 1$ and when p=2, the Minkowski distance so-called Euclidean distance.

In fact, the Euclidean distance gives an accurate measure because it represents the length of the line segment connecting two different points. However, the cost is relatively high because of the use of the square and the sum of squares. In addition, in some applications, the computing of the straightforward line is not always available. Thus Manhattan can be a good candidate technique. Our aim is to conserve the accuracy while reducing the cost and the complexity as we will see in Sec. 3.4 and Sec. 5.

In fact, τ in (12) was based on equations (10), (11), (13), (14) and (26) that use the Pythagorean theorem; it requires the square function. The new comparison will be given through the following equation

$$\tau_p = \sum_{j \in \mathbb{A}} |\tilde{d}_j - \tilde{d}_{jp}| \quad , \tag{16}$$

where p represents an estimate point in a given iteration, and $\tilde{d}_{jp}$ denotes the estimated distance between anchor node j and an estimate point p. This later distance will be computed using a modified Manhattan instead of the squared Euclidean distance, that was utilized in the basic elimination process, as follows.

$$\tilde{d}_{jp} = \tilde{d}_{X_{jp}} + \tilde{d}_{Y_{jp}} + \theta |\tilde{d}_{X_{jp}} - \tilde{d}_{Y_{jp}}| \tag{17}$$

where $\tilde{d}_{X_{jp}} = x_j - x_p$ and $\tilde{d}_{Y_{jp}} = y_j - y_p$ and θ is a real constant. The first and the second terms in (17) represent Manhattan distance and the third term represents a corrective factor that will ensure a higher accuracy level of the comparison. That is, Manhattan gives sometimes wrong estimations as we explain in the following examples where our modified Manhattan gives more accurate comparison results. We will prove in the next sub-sections that a very good value to θ can be 1/2. Therefore, MM with $\theta = 1/2$ allows the engineers to replace the square and root functions by simple shift process (dividing over two in a binary representation). This will dramatically save computational resources needed through the iteration of the elimination process. We will demonstrate through some examples and through intensive simulation hereafter this later outcome.

Let us consider now a first scenario where the differences from an Anchor node j, that is participating in an elimination process, and two estimate points p_1 and p_2 are (2,6) and (4,4). We consider also that $\theta = 0.5$. The estimate point p_2 is closer than p_1 to the anchor node j because the Euclidean distances between j from one side and p_1 and p_2 from the other side are derived from the

Pythagorean theorem and calculated as $\sqrt[2]{4+36}$ and $\sqrt[2]{16+16}$ respectively. Using the Manhattan formula, these distances are equivalent because $\tilde{d}_{jp_1} = 2+6 = 8$ and $\tilde{d}_{jp_2} = 4+4 = 8$. Therefore, Manhattan could not give the right comparison result in this scenario. However, using our formula of modified Manhattan in (17) we find that $\tilde{d}_{jp_1} = 2+6+\frac{4}{2} = 10$ and $\tilde{d}_{jp_2} = 4+4+\frac{0}{2} = 8$, and thus it gives an accurate comparison result without the use of root or square functions. Let us take quickly a second scenario where the differences from j and p_1 and p_2 are (5,7) and (1, 10) and $\theta = 0.5$. The estimate point p_1 is closer than p_2 to the anchor node j because the Euclidean distances are $\sqrt[2]{74}$ and $\sqrt[2]{101}$ respectively. Using the Manhattan formula, we find the opposite result; a wrong estimation. That is, $\tilde{d}_{jp_1} = 12$ and $\tilde{d}_{jp_2} = 11$. Therefore, Manhattan gives again wrong result in another scenario. Now, using our formula of modified Manhattan in (17) we find that $\tilde{d}_{jp_1} = 5+7+\frac{2}{2} = 13$ and $\tilde{d}_{jp_2} = 1+10+\frac{9}{2} = 15.5$, and thus it gives an accurate comparison result.

We show now that Modified Manhattan (MM) gives in some particular scenarios wrong results as Manhattan. We consider the estimate points p_1 and p_2 where the differences from an Anchor node j are (2,5.2915) and (4,4) that are located on the circumference of j (both points are at the same distance of j). The Euclidean distances between j from one side and the estimate points are calculated as $\sqrt[2]{4+28}$ and $\sqrt[2]{16+16}$ respectively. Using the Manhattan formula, the distances are calculated as follows: $\tilde{d}_{jp_1} = 2+5.2915 = 7.2915$ and $\tilde{d}_{jp_2} = 4+4 = 8$. Similar to Manhattan in such a scenario, our formula of modified Manhattan in (17) cannot capture the true result because $\tilde{d}_{jp_1} = 2+5.2915+\frac{3.2915}{2} = 8.9373$ and $\tilde{d}_{jp_2} = 4+4+\frac{0}{2} = 8$ and thus Manhattan (resp. MM) decides that p_1 (resp. p_2) is closer than p_2 (resp. p_1) to j.

In the next Section, we will first evaluate analytically the comparison accuracy of our proposed MM formula as function of θ. We will quantify the error frequency that is made when using MM instead of the Euclidean distance (the square used to compute τ in (12)). Second, we will compare through simulation the relative error made by MM with respect to that made by Manhattan.

Fortunately , the elimination process does not depend on a single comparison result from one Anchor node. In Equ. (16), τ_p depends on the comparison results of at least two Anchor nodes. We will demonstrate through simulation in Sec. 5, that addresses the validation and the performance evaluation of the overall optimized TALS, that the optimized elimination process ensures a very good accuracy with less complexity than the basic process and other localization algorithms found in the literature (to the best of our knowledge).

3.4. Accuracy Evaluation of the Modified Manhattan technique

We will now evaluate the accuracy of our enhanced version of the elimination process analytically and using intensive simulation through Matlab that will help to better understand the impact of the wrong result on the localization process.

3.4.1. Analytic analysis

Consider two points $A = (a, b)$ and $B = (c, d)$. We know that A is closer (resp. farther) from the origin $(0, 0)$ than B if $a^2 + b^2 < c^2 + d^2$ (resp. $a^2 + b^2 > c^2 + d^2$).

Question: when do we make a mistake if we replace the above criterion by the criterion "A is closer (resp. farther) from the origin than B if $a + b + \theta|a - b| < c + d + \theta|c - d|$ (resp. $a + b + \theta|a - b| > c + d + \theta|c - d|$) with $\theta \geq 0$?

Define $X := a^2 + b^2 - (c^2 + d^2)$ and $Y := a + b - (c + d)$.

It is easily seen that $X < 0$, or equivalently A is closer than B from the origin, if and only if

$$Y < \frac{2(ab - cd)}{a + b + c + d}. \tag{18}$$

We therefore need to compare the criterion in (18) to the criterion

$$Y < \theta|c - d| - \theta|a - b|. \tag{19}$$

With (18) and (19) the answer to the question above is easy.

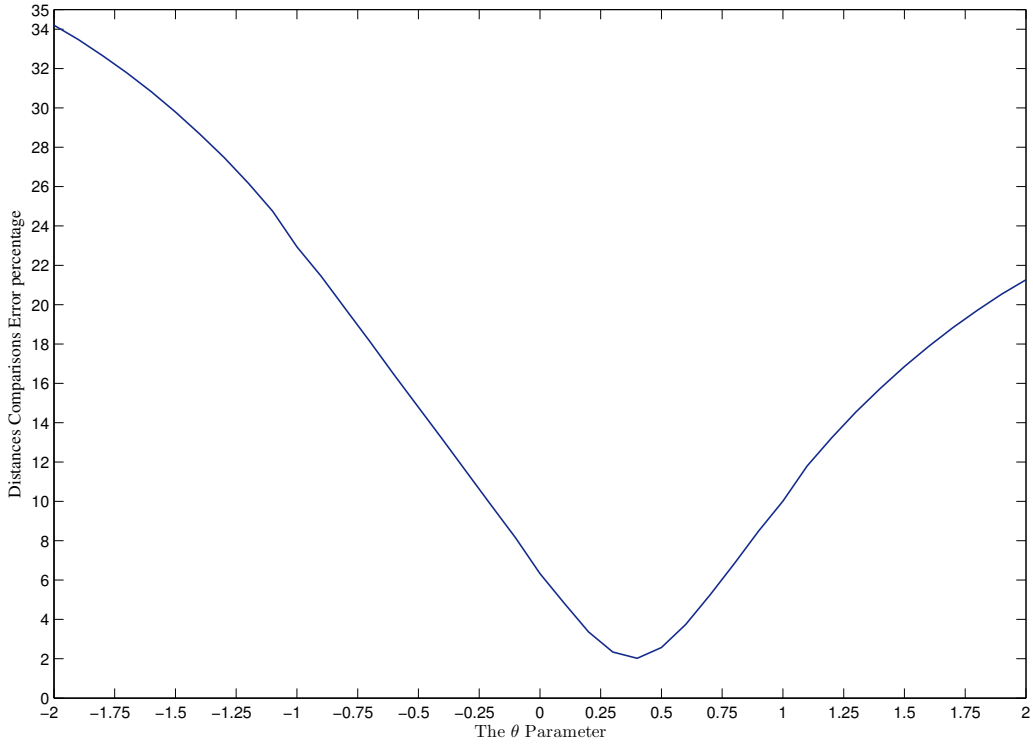

Figure 3: Analysis of Accuracy of Modified Manhattan as function of θ.

If $\theta|c-d| - \theta|a-b| < \frac{2(ab-cd)}{a+b+c+d}$ then using criterion (19) will give the wrong answer for all points A and B such that $\theta|c-d| - \theta|a-b| < Y < \frac{2(ab-cd)}{a+b+c+d}$. Similarly, if $\theta|c-d| - \theta|a-b| > \frac{2(ab-cd)}{a+b+c+d}$ then using criterion (19) will give the wrong answer for all points A and B such that $\frac{2(ab-cd)}{a+b+c+d} < Y < \theta|c-d| - \theta|a-b|$.

In summary, criterion (19) will give the wrong answer for all points A and B such that

$$\min\left(\theta(|c-d|-|a-b|), \frac{2(ab-cd)}{a+b+c+d}\right) < Y < \max\left(\theta(|c-d|-|a-b|), \frac{2(ab-cd)}{a+b+c+d}\right).$$

Let us now quantify the error that is made when using the criterion (19) instead of the Eucledian distance. To do that, consider a square of size 1 and let us calculate the ratio $R(\theta)$ of pair of points in this square for which criterion (19) will return a wrong answer.

We have (with $A = (x, y)$, $B = (u, v)$)

$$\begin{aligned} R(\theta) &= \int_{x=0}^{1}\int_{y=0}^{1}\int_{u=0}^{1}\int_{v=0}^{1} dx\, dy\, du\, dv\, 1\left(\min\left(\theta(|u-v|-|x-y|), \frac{2(xy-uv)}{x+y+u+v}\right)\right. \\ &\quad \left. < x+y-(u+v) < \max\left(\theta(|u-v|-|x-y|), \frac{2(xy-uv)}{x+y+u+v}\right)\right). \end{aligned}$$

Fig. 3 shows the ratio $R(\theta)$ for $\theta = -2 : 0.1 : 2$. We notice that the best value of θ is equal to 0.4 (It corresponds to 2.0232% of error that is the minimum). However, from practical point of view, setting the value of θ to 0.5 (The second best value that corresponds to 2.574% of error) allows the engineers to replace the complex computations (roots, square, multiplication , division, etc)

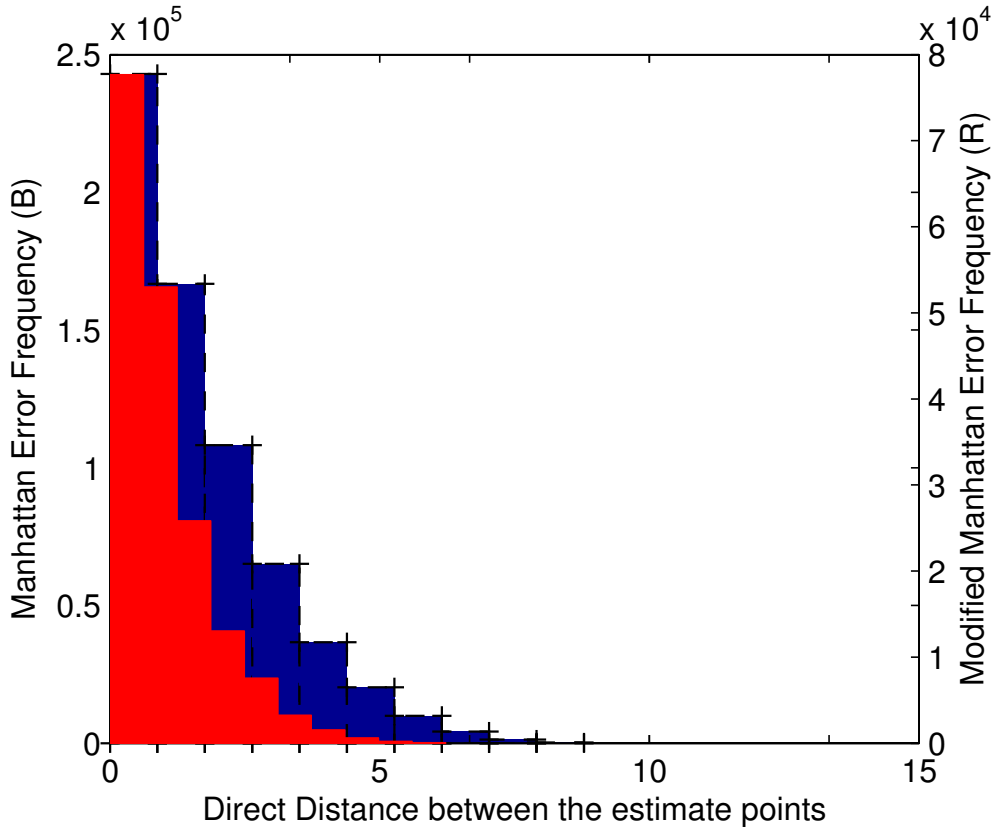

Figure 4: Comparison between Modified Manhattan and Manhattan distances.

by a simple shift process (dividing over two in a binary representation) with a minor additional comparison error. Note that the MM becomes Manhattan when $\theta = 0$. From Fig. 3 we see that Manhattan gives 6.325% of wrong results.

3.4.2. Simulation result

We now evaluate the accuracy of our enhanced version of the elimination process using intensive simulation through Matlab while considering $\theta = 0.5$. We assume a square area of dimensions 31x31 measurement unit, e.g. m. We take 10218313 random possible locations of two estimate points around an anchor node. The total numbers of the wrong estimations using Manhattan and Modified Manhattan are 623320 and 194704 respectively. The relative errors for both techniques are 6.1% and 1.91% respectively. To understand the reason of the wrong estimations, we first maintain two arrays of length equal to the number of wrong estimations using the Manhattan method and the Modified Manhattan method respectively. The value of each element in both arrays correspond to the absolute difference between the straight-line distances of the estimate points to the anchor node. Then, we draw the histogram of those two arrays that shows the error frequency of the estimation result in both Manhattan and our modified Manhattan techniques with respect to differences between the straight-line distances of the estimate points as demonstrated in Fig. 4. We notice from the figure that the high error frequency occurs when the difference between the straight-line distances of the estimate points to the anchor node is equal to zero, and then to one and two (the estimate points are at the same distance or close to be at the same distance from the anchor node). In fact, with very high probability, this happen in the last iteration phases of the elimination process where the estimate nodes become so close to the right position, and then even if a wrong estimation is made by MM, a very close position is already found. However, and this is a very important remark, when both estimate points are from one distance of one anchor node, they

will be with high probability at different straight-line distances from the second anchor nodes that participate in the elimination process. Therefor, the error frequency of the elimination process that depends on the comparison results from at least two Anchor nodes as shown in Eq. (16) will be reduced as we will see in Sec. 5. We conclude from the analysis and simulation results that the modified Manhattan is very efficient for hardware of embedded system environment of WSN. It avoids the multiply operations used to get the square of a number in the calculation of the distance between two nodes similar to Manhattan. In addition, it is more accurate than the Manhattan distance and less complex than the Euclidean technique and the other methods appeared in the literature, that require basically solving a linear system of equations via least square or its variant.

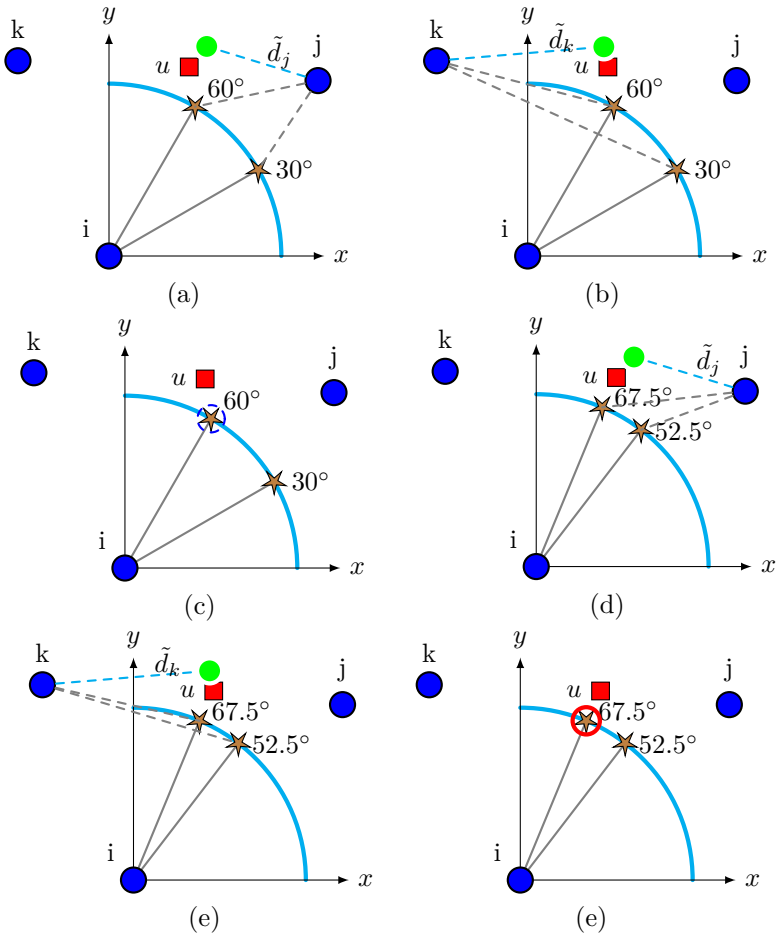

Figure 5: Example of the second iteration phase in TALS elimination process.

3.5. Selection of base anchor

In this section, we show how a base anchor is selected. Initially, the ordinary node u that is not localized yet finds n, the surroundings anchors within its transmission range Γ as in Fig. 2(a). Only if ($n > 2$), node u will start the localization process by selecting one of its surroundings anchors as its base. The highest priority of neighbor anchors to be a base will be given to the fixed anchors. Now, we define two methods to select a base Anchor and describe each one in details. The two methods differ in the computational complexity and storage space.

Method 1: Selecting one base anchor randomly from all neighbor anchors. Fig. 2 shows an example in which node u chooses anchor node i to be its base anchor and then starts to compare the estimated positions on the base anchor circle circumference with radius $\tilde{d}_i$ to the distance

from the other anchor nodes j and k. Random selection may be useful for wireless networks with nodes having low computational power. However, it may result in significant errors in selecting the quarter at the elimination process as we will see in Sec. 4.1.

Method 2: Repeat method one with each anchor, considering one anchor as a base at a time, then selecting the one that leads to the lowest residual. This means that the selection process repeats for all anchor nodes where the next anchor will act as a base and the remaining anchors will aid in the localization process. This way for each anchor node received by the localizing node, an estimate will be produced. This redundancy will be of a great benefit where fusion techniques can be employed to combine the estimate into an accurate location as shown in Sec. 3.6.

Note that in case the sensor is surrounded by more than three anchors we can consider taking r anchors at a time where $(3 < r \leq n)$, where n is the maximum number of Anchor nodes in the range of the given sensor. In this case the total number of the combinations is $(\sum_{i=3}^{n} {}^{n}C_i)$. a key issue to be considered is the simplicity of the localization algorithm because it is crucial for implementation and efficiency purposes.

3.6. Data Fusion Technique and Accuracy Enhancement

As shown in Sec. 3.5, TALS repeats the location selection procedure for each anchor node by setting them as base nodes one at a time. Thus, for each anchor node location received, an estimate for the node being localized is calculated. This redundancy enhances the quality of the estimates and eliminates diverging measurements to a great extent. Since TALS computes the locations of the nodes iteratively, weights can be assigned to add confidence to anchor nodes. The first step in TALS algorithm starts by anchor nodes broadcasting their locations. Each node that receives more than three anchor nodes' location can start the estimation process of its own location. These nodes are upgraded to virtual Anchor node status and broadcast their locations to neighboring nodes and the localization process continues until all nodes are localized. Confidence is given according to two parameters: the number of fixed or virtual anchor nodes and the distance to the node being localized. Higher confidence is given for fixed anchor nodes since they have accurate positions. Thus, given the list of anchors (fixed and virtual), the probabilistic weight is given according to equation (20) where ϕ represents an empty set.

$$w_a(i) = \begin{cases} \frac{0.75}{\text{Total\_F Anchors}}, & \text{if\{i=}F_{anchor}\text{\}\&\{}V_{anchor} \neq \phi\text{\}} \\ \frac{1}{\text{Total\_F Anchors}}, & \text{if\{i=}F_{anchor}\text{\}\&\{}V_{anchor} = \phi\text{\}} \\ \frac{0.25}{\text{Total\_V Anchors}}, & \text{if\{i=}V_{anchor}\text{\}\&\{}F_{anchor} \neq \phi\text{\}} \\ \frac{1}{\text{Total\_F Anchors}}, & \text{if\{i=}V_{anchor}\text{\}\&\{}F_{anchor} = \phi\text{\}} \end{cases} \tag{20}$$

As shown in equation (20), each anchor node belonging to the localizing node's list of anchor nodes is assigned a probabilistic weight w_a according to its status. The value 0.75 in the equation means multiply by 3 and divide by 4, which is 2 shift operations in binary representation and not a real division. Thus, we keep the simplicity of the low computation cost of TALS. In fact, if the anchor node's list contains only fixed or virtual anchor nodes, each anchor node will receive equal weight assignment. On the other hand, if the anchor list contains mixed fixed and virtual anchors, fixed anchor nodes are assigned higher weights than virtual anchors since the latter can have inaccuracies about their estimated positions. Moreover, low estimated ranges from the base anchor node to the node being localized should be assigned high weights since low ranges minimize errors. In this context, given the distance from the base anchor node to the node being localized d_i and the maximum transmission range Γ, the probabilistic weight w_d is assigned according to equation (21). Consequently, each estimate computed from each anchor node is assigned the normalized weight w_{dN} as shown in equation (22).

$$w_d(i) = 1 - \frac{d_i}{\gamma} \tag{21}$$

$$w_{dN}(i) = \frac{w_d(i)}{\sum_{j=1}^{n\_anchors} w_d(j)} \tag{22}$$

Since w_{dN} and w_a are independent, their joint probability distribution is given by (23). The final weight assigned for each estimate generated by an anchor node is given by (24). The final estimate is given by equation (25).

$$P(w_{dN}(i), w_a(i)) = w_{dN}(i) \times w_a(i) \tag{23}$$

$$w(i) = \frac{P(w_{dN}(i), w_a(i))}{\sum_{j=1}^{n\_anchors} P(w_{dN}(j), w_a(j))} \tag{24}$$

$$(\tilde{x}, \tilde{y}) = \sum_{i=1}^{n\_anchors} w(i) \times (\tilde{x}_i, \tilde{y}_i) \tag{25}$$

4. Analysis

In this section, we study analytically the effect of different parameters of the optimized TALS on the localization process. Additional parameters that are difficult to analytically formulate them are studied using simulation.

4.1. Accuracy of Quarter Selection

As stated before the elimination process starts by choosing which quadrant the estimate lies on. The algorithm starts initially by selecting four points which lie on the circle of node i at 45° from the x-axis. The point that has the lowest residue resulting from taking the sum of absolute differences is the point that is the nearest to the node and hence the quadrant is selected. Next, we show by example that this step may lead to wrong quadrant although anchors nodes do not lie on a straight line. However, by deployment of Method 2 discussed in the previous section or applying a data fusion technique (presented in Sec. 3.6), we can easily address this possible wrong estimation.

4.1.1. Example of wrong estimation

Figure 6 gives an example for the output of the basic TALS algorithm. In the figure, there are three Anchors $j; k; l$. The transmission range is fixed to 35 unite. The figure shows an example of the wrong estimation of the Quarter although anchors nodes are not collinear. The node actually lie in quadrant IV and TALS evaluates it wrongly to lie in quadrant I.

4.2. Analysis of the effect of Degree of Divisions and Threshold Selection

The degree of divisions δ is defined as the smallest angle with which the iterative division of the circle of the base anchor node is achieved. For example, the case shown in Fig. 1(b) has the smallest angle δ set to 7.5°. The number of estimate points κ is given by $\kappa = \frac{360}{\delta}$. The selection of δ depends on an acceptable estimation error which is an application based parameter. Finer granularity of δ will yield lower error which comes at the cost of increasing the iterative computations because the number of the elimination phases increases. Therefore, δ is related with the threshold ξ. We said in Sec. 3.1 that if at any time the residual τ is smaller or equal to the threshold ξ, the elimination process stops and the point with the lowest residual is selected as the final estimate. For that, the selection of the threshold ξ depends on two parameters: the degree of division δ and the maximum transmission range Γ. Higher ranges will yield larger radii which translate to bigger pores between the estimated points. The threshold selection is bounded by equation (26) which is given by Theorem 1 that is presented and proofed by Merhi et. al. in [7].

Theorem 1. Given no errors are introduced on the ranging measurements between the localizing node and the anchor node in a one hop scenario, the maximum error is bounded by equation (26):

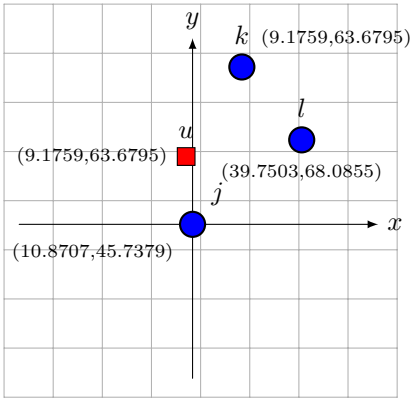

(a)

Figure 6: Example for wrong Quadrant selection in the basic TALS.

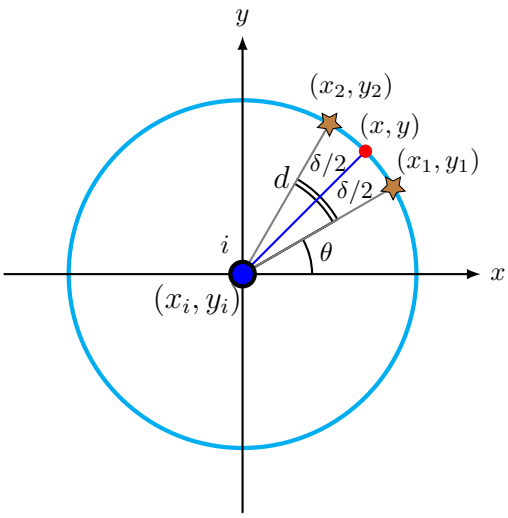

Figure 7: Maximum error in a one-hop scenario.

$$\xi_{max} = \Gamma\sqrt{2(1 - cos(\frac{\delta}{2}))} \tag{26}$$

Where Γ is the maximum transmission range and δ is the degree of division.

4.3. Optimization for TALS

We have seen that a trade-off between a small degree of division δ and the computation cost is needed in order to assure a good accuracy level of the algorithm while keeping low computation cost and storage space.

In fact, the sine and cosine operations used to determine the estimate points shown in equations (1) and (2) have non negligible computation cost. Since these divisions are static, the sine and cosine values can be stored in a lookup table. In the view of the fact that the four quadrants act like mirrors to each other, only 1/4 of the table entries need to be stored. In addition, equations (27) and (28) shows that only one entriy is needed for the sine or the cosine functions. Thus, we need $\kappa = \frac{0.25 * 360}{\delta}$. If $\delta = 7.5$, we need only 12 entries.

$$cos(\alpha) = sin(90 - \alpha) \tag{27}$$

$$sin(\alpha) = cos(90 - \alpha) \tag{28}$$

5. Validation and Performance Evaluation of the optimized TALS

The performance of the TALS localization system is evaluated through a stochastic simulation study. All the simulations scenarios are carried out in MATLAB. This section presents the simulation environment, and the parameters of the evaluation.

5.1. Simulation settings

In our simulation, we assumed squares deployment areas with sides length 100x100 and 500x500 grid unit. We used a standard uniform pseudo-random generator to distribute sensors in the deployment area. Note that there are no restrictions on the places where sensor can be placed, it can be placed at any grid point. We run several simulation experiments using different sensor densities (from 80 up to 250 sensors) in the deployment areas and different percentage of the Anchor nodes (from 5% up to 80%). In order to mitigate the randomness, we repeat each experiment 100 times and report the average of the outputs. We stop the simulation when all the nodes having enough neighbor anchors (or virtual anchor) nodes are localized. We consider scenarios with and without noisy range measurements. We assume in some scenarios nodes with homogeneous transmission range of 20, 25 and 35 distance units and in other scenarios with heterogeneous transmission ranges randomly assigned between 5 and 35 distance units. We estimated localization error as the average of the Euclidean distance between the actual and the estimated positions of sensors. Mathematically, this was expressed as,

$$Avg.Error = \frac{\sum_{i=1}^{u} \sqrt{(\tilde{x}_i - x_i)^2 + (\tilde{y}_i - y_i)^2}}{u} \tag{29}$$

where u is the number of ordinary nodes, $(\tilde{x}_i, \tilde{y}_i)$ is the estimated node position, and (x_i, y_i) is the actual node position. In all experiments and for any base node i, the degree of division δ is set to 7.5°.

5.2. Validation of optimized TALS

We will validate the global functionality of TALS and show how TALS gives very accurate results in different scenarios. As the computation cost of TALS is minimized with respect to the known localization systems as explained in Sec. 2 and 3.3, TALS is a promising localization system for WSN. It is worth mentioning that in the previous joint work, Merhi et. al. presented a comparison between the basic TALS System [7], Multilateration [6] and the 7 point trilateration [32] as a function of errors introduced on ranging measurements. TALS performance is superior to all other techniques for all error ranges. We focus hereafter on the accuracy and the performance evaluation of the optimized TALS with respect to the different system parameters.

Figure 8 shows an example of regular WSN topology in a deployment area of 500x500 units and 250 sensors. The number of Anchors is 50 nodes (20%). The transmission range is randomly distributed between (10 and 35 unites) and we don not consider noise in the transmission measurements. The figure shows the comparison result between the exact and estimated locations of sensors. We can notice how good it is the accuracy of TALS (96% of the estimated locations overlap the exact ones). For this scenario, we calculated the absolute estimation error vector as the difference between the distance of the exact position of unlocalized nodes to the center and the distance of the estimated position to the center. We reported the mean value of the error and the variance and we depict in Fig. 9 the histogram of this metric. The mean value of the error is 0.3162 measurement unit and the variance is 4.7349 measurement unit. It is clear from

the histogram that 246 sensor out of 250 are localized with absolute estimation error less than 2.5 measurement unit.

Figure 10 shows a different scenario where the grid is 100X100 units and the density is 80 sensors with only 10% Anchors (8 Anchors) with transmission range between (5 and 35 unites). The unlocalized nodes that have enough Anchor neighbors (3 at least), will become later virtual Anchors and will aid in the localization process of the others. It is clear that TALS is a very good algorithm even with small number of initial Anchors.

In the following sections, we will examine carefully the effects of different parameters on the overall performance.

5.3. Effect of Anchor density

The anchor ratio is one of the most important factors affecting localization accuracy. Thus, we report accuracy and performance results with a varying number of anchor nodes. Since the ratio of the anchor nodes is controlled by the fixed number of sensor nodes deployed in the sensor field, the number of normal nodes is decreased if the number of anchor nodes is increased. In this case we are more interested in the performance when the anchor ratio is small because in a practical system the number of anchor nodes will be much lower than the number of unlocalized nodes. Figure 11 shows that different anchor ratios will influence the amount of location errors. One can see that with the same node density at the same deployment area, when the percentage of initial anchors is increased from 20% to 30%, the average localization errors decrease significantly. Our algorithm performs well as it manages to produce small error, even without large numbers of Fixed anchors as clearly shown also in Fig. 10.

5.4. Effect of Node density

Our second goal from the simulation is to determine the effect of node density on the localization success ratio and the average of localization error. For this experiment, we gradually increase the number of nodes from 80 to 220 in the same network area. As the number of nodes grows, the node density increases, and the number of derived anchors increases too. As depicted in Fig. 11(a), we found that as we increase the node density, the localization success ratio gets higher as expected. The question that has been answered here is: what is a good initial fixed anchor ratio to achieve certain accuracy level or localization error. We conclude that nodes benefit from more neighbors and redundancy. Also, that the error propagation of ordinary nodes becoming derived anchors and aiding other nodes in the localization process are within acceptable range.

5.5. Localization under noisy distance measurements

In this simulations, the noisy range measurements are generated randomly and the distance error variation has a maximum of 5% of the actual distance between nodes. As shown in Fig. 11(b), the localization error is plotted against the ranging measurements error. With the increase of ranging errors, the localization accuracy is affected. However, with small noise range measurements, the influence is still negligible in the proposed optimized TALS contradicting many known localization systems.

5.6. Impact of transmission range

Figure 12 shows that TALS performs better at high transmission ranges where the unlocalized nodes benefiting from more Fixed and Virtual Anchors. The percentage of Fixed anchor nodes is kept fixed at 20% and the transmission range in the simulation varies between 10–50 units. Note that for the smallest transmission range available (10 units), the average error is small because many nodes will not be localized (less than three Anchor or virtual neighbors nodes are found) and has no error to be counted. With larger transmission range, more nodes (and potentially all) will be localized and their errors will start to be counted. However, as we increase the transmission range (above the value that permits most nodes to be localized), average localization error decreases. In addition, with the increase of the network density, the error decrease in a slow rate.

5.6.1. Localization of non-convex networks

Finally, we evaluate TALS in non-convex networks. Figure 13 illustrates two instances. The sensors are randomly deployed in a H-shaped, and C-shaped region, respectively. We repeat the simulations and the results are consistent to show the applicability and efficiency of TALS in localization of non-convex networks as shown in Fiq. 14.

6. CONCLUSION

In this work, a novel low complexity anchor based range based localization system based on trigonometric identities and properties that we have recently proposed is intensively analyzed and different optimization techniques are utilized. The optimized TALS is tailored to suit wireless sensor network environment where the contributions made can be summarized as follows:

- TALS is designed to have a low computational overhead where it does not require solving a linear system of equations via least square or its variant as in many known studies. The optimized TALS doest not also require any square root operation or least square approximations thanks to the deployment of the modified Manhattan technique that leads to the avoidance of the multiply operations used to get the square of a number in the calculation of the distance between two nodes (as in the basic TALS). The optimized TALS ensures a very good accuracy and less complexity compared to the basic TALS and other methods appeared in the literature. Thus, the optimized TALS is very efficient for hardware implementation of embedded system environment of WSN.
- The system does not require any flooding mechanism which saves communication bandwidth and power.
- TALS takes advantage of redundancy to enhance the quality of the estimate by employing data fusion techniques. Furthermore, a novel data fusion technique is presented which analyzes the number of fixed and virtual anchor nodes and the distance from the node to the anchor nodes to assign weights accordingly which yield a better estimate.
- Correct and accurate equations formulas of the basic TALS system are presented and several optimizations concerning the effects of degree of divisions and threshold were performed on TALS to speed up the execution, reduce computations and decrease storage requirements.
- A deep analysis, and extensive simulation of the optimized TALS are presented while showing its cost, accuracy, efficiency, and deducing the impact of its parameters on the performance.

In future, we plan to adapt and evaluate the optimized TALS to the 3D-localization problems and to consider the sensors mobility and asses its impact on exchanging data and the performance based on previous joint works such as [10, 34] and [35].

Acknowledgement

We would like to thank Dr Philippe Nain from INRIA-Sophia Antipolis for his advice and assistance concerning the analysis of Modified Manhattan and other helpful technical discussions.

References

[1] L. Zou, M. Lu, Z. Xiong, Pager-m: A novel location-based routing protocol for mobile sensor networks, in: Proceedings of First International Workshop on Broadband Wireless Services and Applications, San Jose, CA, 2004.

[2] J. Elson, L. Girod, D. Estrin, Fine-grained network time synchronization using reference broadcasts, in: SIGOPS Oper. Syst. Rev., Vol. 36(SI), 2002, pp. 147–163.

[3] B. Kusy, P. Dutta, P. Levis, M. Maroti, A. Ledeczi, Elapsed time on arrival: a simple and versatile primitive for canonical time synchronization services 2 (1).

[4] I. Amundson, X. D. Koutsoukos, A survey on localization for mobile wireless sensor networks, MELT 2009, LNCS 5801 (2009) 235–254.

[5] D. Niculescu, B. Nath, Ad hoc positioning system (aps), in: proc. of GLOBECOM, Vol. 5, IEEE, 2001, pp. 2926–2931.

[6] A. Savvides, C. C. Han, M. Strivastava, Dynamic fine-grained localization in ad-hoc networks of sensors, in: In Proceedings of the 7 th annual international conference on Mobile computing and networking, Vol. 2001, 2001, pp. 166–179.

[7] Z. Merhi, M. Elgamel, R. Ayoubi, M. Bayoumi, Tals: Trigonometry-based ad-hoc localization system for wireless sensor networks, in: In IWCMC 2011, 7th International Wireless Communications and Mobile Computing Conference, IEEE, 2011, pp. 59–64.

[8] P. Volgyesi, G. Balogh, A. Nadas, C. Nash, A. Ledeczi, Shooter localization and weapon classification with soldier-wearable networked sensors, in: in Proceedings of MobiSys (2007) the 5th International Conference on Mobile Systems, Applications, and Services, 2007.

[9] J. Eriksson, L. Girod, B. Hull, R. Newton, S. Madden, H. Balakrishnan, The pothole patrol: using a mobile sensor network for road surface monitoring, in: Proceedings of MobiSys (2008) the 6th international conference on Mobile systems, applications, and services, 2008.

[10] A. A. Hanbali, A. A. Kherani, R. Groenevelt, P. Nain, E. Altman, Impact of mobility on the performance of relaying in ad hoc networks - extended version, Computer Networks 51 (14) (2007) 4112–4130.

[11] P. Volgyesi, A. Nadas, X. Koutsoukos, A. Ledeczi, Air quality monitoring with sensormap, in: Proceedings of the 7th international conference on Information processing in sensor networks (IPSN 2008), 2008, pp. 529–530.

[12] N. B. Priyantha, A. Chakraborty, H. Balakrishnan, The cricket location-support system, in: In Proceedings of the 6th annual international conference on Mobile computing and networking, ACM, 2000, pp. 32–43.

[13] X. Qu, L. Xie, Source localization by tdoa with random sensor position errors—part i: static sensors, in: in Proceedings of the 15th International Conference on Information Fusion, Singapore, 2012, pp. 48–53.

[14] K. C. Ho, Bias reduction for an explicit solution of source localization using tdoa 60 (5) (2012) 2101–2114.

[15] X. Qu, L. Xie, Source localization by tdoa with random sensor position errors—part ii: mobile sensors, in: in Proceedings of the 15th International Conference on Information Fusion, Singapore, 2012, pp. 54–59.

[16] D. Niculescu, B. Nath, Ad hoc positioning system (aps) using aoa, in: INFOCOM 2003. Twenty-Second Annual Joint Conference of the IEEE Computer and Communications, Vol. 3, IEEE, Atlanta, GA, 2003, pp. 1734–1743.

[17] Y. M., A. A., The horus location determination system 14 (3) (2008) 357–374.

[18] P. Motter, R. Allgayer, I. Müller, E. Freitas, Practical issues in wireless sensor network localization systems using received signal strength indication, in: IEEE Sensors Applications Symposium, IEEE, San Antonio, 2011, pp. 227–232.

[19] L. Cheng, C. D. Wu, Y. Z. Zhang, Y. Wang, Indoor robot localization based on wireless sensor networks 57 (3) (2011) 1099–1104.

[20] K. Lu, X. Xiang, D. Zhang, R. Mao, Y. Feng, Localization algorithm based on maximum a posteriori in wireless sensor networks 2012 (ID260302) (2012) 1099–1104.

[21] G. Mao, B. Fidan, B. .Anderson, Wireless sensor network localization techniques, 2007.

[22] D. Niculescu, B. Nath, Dv based positioning in ad hoc networks, in: in Journal of Telecommunication Systems, Vol. 22, 2003, pp. 267–280.

[23] S. W. Lee, D. Y. Lee, C. W. Lee, Enhanced dv-hop algorithm with reduced hop-size error in ad hoc networks 94 (7) (2011) 2130–2132.

[24] C. Huang, B. M. Blum, A. ahmed, J. A. Stankovic, T. Abdelzaher, Range-free localization schemes for large scale sensor networks, 2003.

[25] N. B. J., J. Heidemann, D. Estrin, Gps-less low cost outdoor localization for very small devices, IEEE Personal Communications Magazine 7 (2000) 28–34.

[26] Y. S. University, Y. Shang, Localization from mere connectivity, in: Fourth International ACM Symposium on Mobile Ad Hoc Networking and Computing, 2003.

[27] M. A., F. M., L. N., Wireless sensor networks localization algorithms: a comprehensive survey., International Journal of Computer Networks and Communications (IJCNC) 5 (6).

[28] L. Cheng, C. D. Wu, Y. Z. Zhang, H. Wu, M. Li, C. Maple, A survey of localization in wireless sensor network 2012 (ID 962523) (2012) 1099–1104.

[29] W. Parkinson, P. Enge, P. Axelrad, J. J. Spilker, Global Positioning System: Theory and Application, VOLUME II, Vol. 163, 1996.

[30] G. W. H., Z. C., Econometric analysis, Vol. 3, Prentice Hall, New Jersey, 1997.

[31] G. S. Kuruoglu, M. Erol, S. Oktug, Localization in wireless sensor networks with range measurement errors, in: In Proceedings of AICT 2009, Fifth Advanced International Conference on Telecommunications, Venice, 2009, pp. 261–266.

[32] Z. Merhi, M. Elgamel, M. Bayoumi, A lightweight collaborative fault tolerant target localization system for wireless sensor networks 12 (8) (2009) 1690–1704.

[33] J. Niu, B. Lu, L. Cheng, Y. Gu, L. Shu, Ziloc: Energy efficient wifi fingerprint-based localization with low-power radio, in: 2013 IEEE Wireless Communications and Networking Conference WCNC, 2013, pp. 4558–4563.

[34] S. Alouf, F. Huet, P. Nain, Forwarders vs. centralized server: an evaluation of two approaches for locating mobile agents, Perform. Eval. 49 (1/4) (2002) 299–319.

[35] A. A. Hanbali, P. Nain, E. Altman, Performance of ad hoc networks with two-hop relay routing and limited packet lifetime (extended version), Perform. Eval. 65 (6-7) (2008) 463–483.

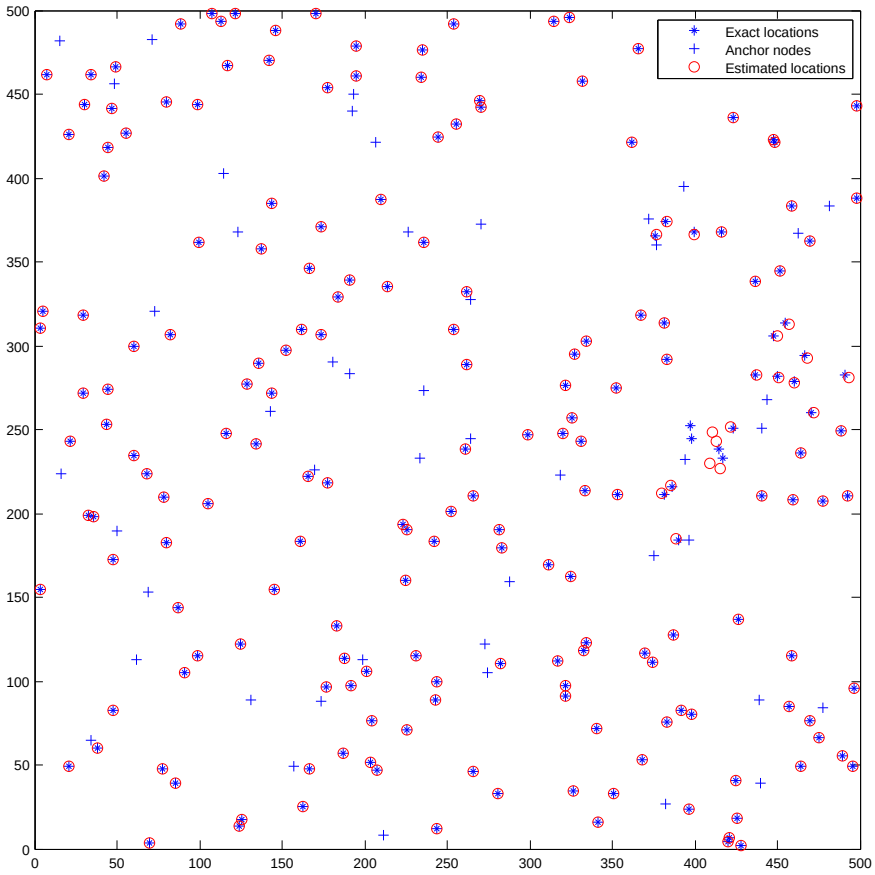

Figure 8: Comparison between exact and estimated sensors location. 500x500 grid, 250 sensors with 20% Anchors (50), Random transmission ranges (10–35)

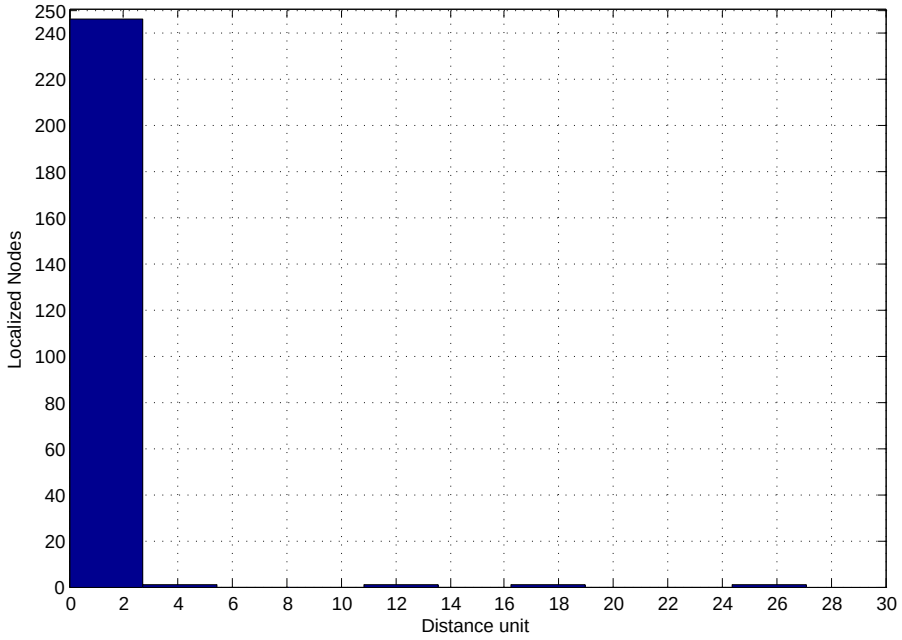

Figure 9: Histogram of the absolute error between the distance of exact and estimated sensors location to the center. 500x500 grid, 250 sensors with 20% Anchors (50), Random transmission ranges (10–35)

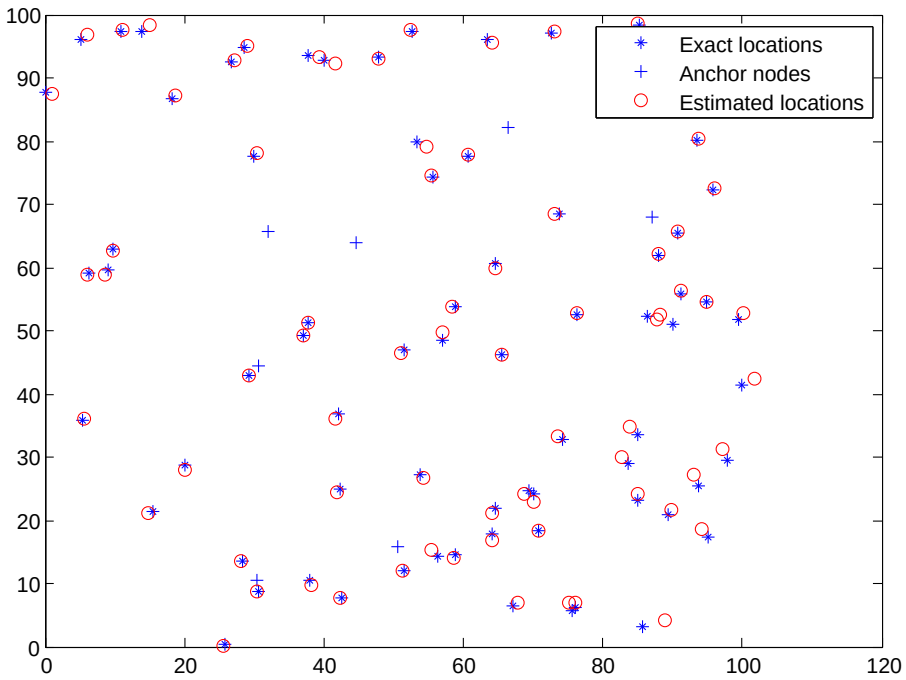

Figure 10: Comparison between exact and estimated sensors location. 100x100 grid, 80 sensors with 10% Anchors (8), Random transmission ranges (5–35)

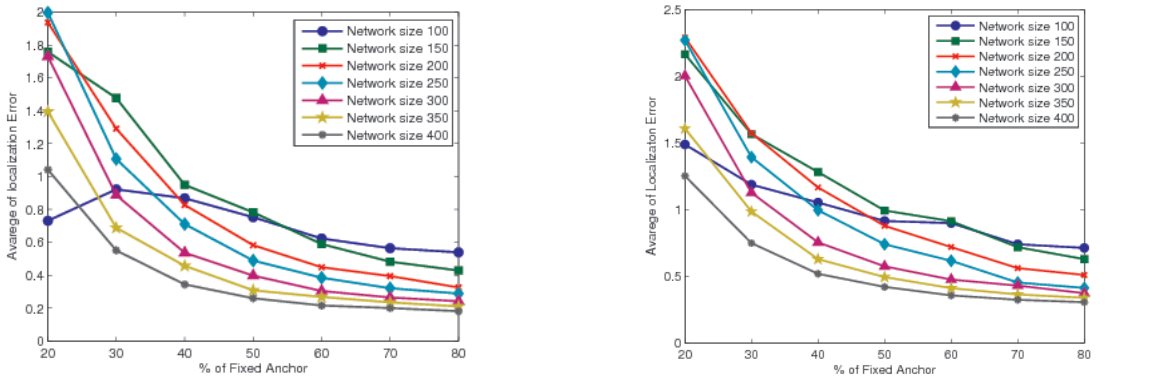

(a) Average position error without noise interference (b) Average position error with noise interference

Figure 11: Effect of number of Fixed Anchors under different node densities on localization error.

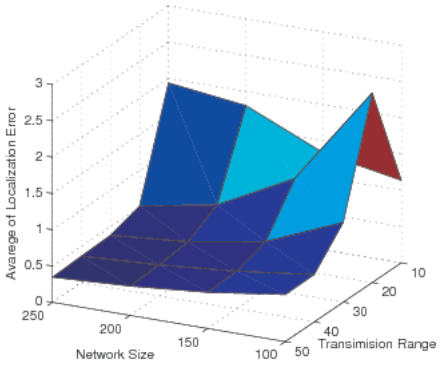

Figure 12: Localization success vs. Network size and Transmission range.

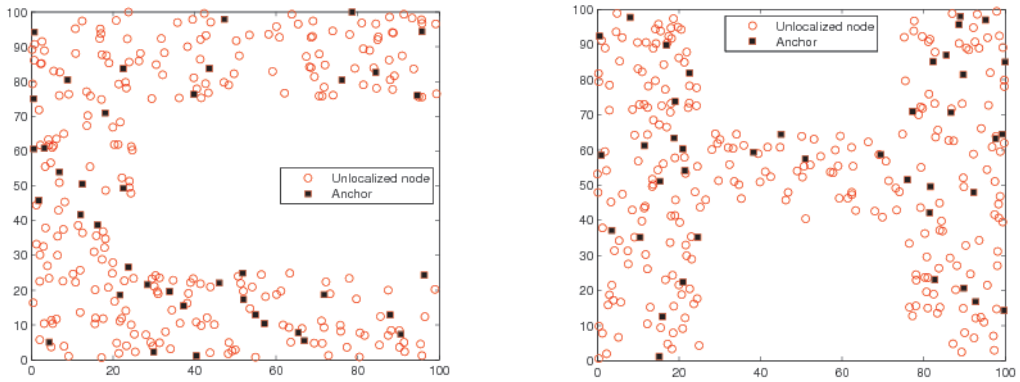

(a) (b)

Figure 13: Irregularly-Shaped non-convex Networks. (a) Example of C-shaped network topology. (b) Example of H-shaped network topology.

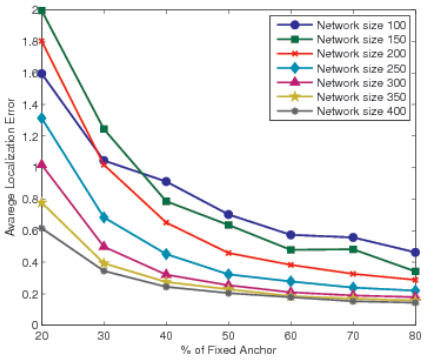

(a) C-shaped network topology

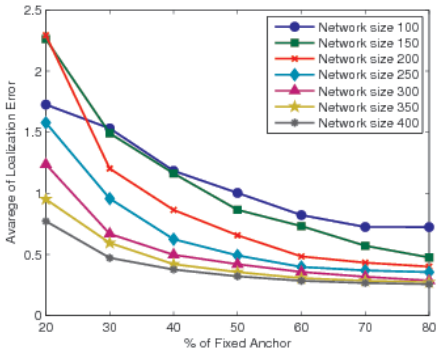

(b) H-shaped network topology

Figure 14: Effect of number of Fixed Anchors under different node density on localization error.